# UNSTEADY MHD CONVECTION OF A RADIATING FLUID PAST A MOVING PERMEABLE VERTICAL PLATE IN A POROUS MEDIUM

Satish Kumar SINGH[1], Daniel Oluwole MAKINDE[2], Adetayo Samuel EEGUNJOBI[3]*

*In the present paper, the authors have considered the unsteady MHD convection of a radiating viscous incompressible electrically conducting fluid past a moving permeable vertical plate maintained at a variable temperature. The governing partial differential equations are obtained and analytically tackled using the Laplace transform technique numerically via the finite difference method. Pertinent results depicting the effects of various emerging parameters on the fluid velocity, temperature profiles, skin friction, and Nusselt number are displayed graphically and in tables. It is found that both skin friction and Nusselt number upsurge with a rise in fluid suction and magnetic field intensity, while a boost in thermal radiation, buoyancy force, and heat source lessened the skin friction and Nusselt number*

**Keywords**: Moving plate, MHD, Unsteady flow, thermal radiation, porous medium, buoyancy force, heat source.

## 1. Introduction

Studying viscous incompressible fluid flow past porous media is fascinating and important in fluid dynamics and porous material science. This complex phenomenon occurs when a viscous fluid hits a media containing linked empty spaces, such as soils, rocks, or biological tissues. Complex flow patterns result from fluid-porous structure interaction, making it of great scientific and practical interest. This fascinating interaction affects groundwater flow through soil in environmental engineering and blood flow through porous tissues in biomedical engineering. Understanding the dynamics of viscous incompressible fluid flow via porous media can solve problems in oil reservoir engineering, filtration, and heat exchanger optimization. Stokes [1] investigated the flow of a viscous incompressible fluid past an impulsively started infinite horizontal flat plate within its own plane. Bassant and Clement [2] investigated the magnetohydrodynamics (MHD) natural

[1] Thakur College of Engineering & Technology Kandivali (East), Mumbai, India, sksdr2010@gmail.com
[2] Faculty of Military Science, Stellenbosch University, Private Bag X2, Saldanha 7395, South Africa, makinded@gmail.com
[3] *Mathematics Department, Namibia University of Science and Technology, Windhoek, Namibia, samdet1@yahoo.com (corresponding author)

convection flow of fluids with different Prandtl numbers in the Stokes problem for a vertical porous plate. The equations are solved semi-analytically using the Laplace transform technique and the Riemann-sum approximation method. The effects of various flow parameters on velocity, temperature, skin friction, and heat transfer rate are discussed with graphs. They extended the scope of earlier results and validated the Riemann-sum approximation method.

Exploring free convection flow, the movement of an electrically conducting fluid against an endless vertical plate is important in many engineering and applied science domains. This research has led to novel MHD accelerators and power generation devices. The study of free convection flow is also important in nuclear reactor cooling, where fluid dynamics are key for heat dissipation. This research contributes to astrophysics by revealing star and planet structure dynamics. Studies of free convection flow past an infinite vertical plate are crucial to solving terrestrial and celestial engineering problems. Reddy and Makinde [3] discussed the impact of Newtonian heating on MHD unsteady free convection boundary layer flow past an oscillating vertical porous plate with thermal radiation, chemical reaction, and heat absorption. The study analyzed dimensionless velocity, temperature, concentration profiles, skin friction coefficient, Nusselt number, and Sherwood number. Results revealed that thermal and mass buoyancy effects support velocity, while increased magnetic field strength had a reverse effect. The concept of model problem holds excellent relevance in engineering and industry, with applications ranging from ceramic and glassware manufacturing to polymer production, food processing, heat exchangers, nuclear power plants, and gas turbines. Sulemana et al. [4] presented a chemically reactive fluid's hydrodynamic boundary layer flow over an exponentially stretching vertical surface with a transverse magnetic field in an unsteady porous medium. They used an approximate analytic method to solve the dimensional partial differential equations, and the results are presented graphically and numerically. They concluded that the controlling parameters effectively reduce skin friction in a chemically reactive magnetic porous medium, which was relevant in practical applications such as solar energy collector systems and material processing.

Eegunjobi and Makinde [5] investigated the effects of various parameters on the unsteady mixed convection flow of an electrically conducting fluid past a stretching sheet in a porous medium. The governing equations were transformed and solved numerically. Their findings unveiled that the augmentation of buoyancy forces resulted in increased heat and mass transfer rates and reduced the thermal and concentration boundary layer density. Ajay et al. [6] investigated the influence of radiation and internal heat generation (absorption) on the dynamics of unsteady laminar natural convective boundary layer flows over a truncated cone. They derived a set of coupled nonlinear partial differential equations by applying appropriate transformations to describe the flow and heat transfer governing

principles. Their numerical results highlighted the substantial impact of pressure work, internal heat generation (absorption), radiation, and magnetic field on skin friction and heat transfer in the system. Comprehensive research investigations encompassing various scenarios have been conducted on viscous incompressible fluid flow, which are detailed in [7-10].

The interaction between MHD and moving plates represents a fascinating and consequential area of study within fluid dynamics. MHD, a discipline at the intersection of magnetism and fluid mechanics, explores the behavior of electrically conducting fluids in the presence of magnetic fields. These are applicable in various scientific and engineering domains, including astrophysics, geophysics, and the design of advanced technological systems. The numerical investigation by Hasanuzzaman et al. [11] explored the effects of thermal diffusion and Dufour on a time-dependent free MHD convective transport flow over an inclined permeable plate. The transformed dimensionless ordinary differential equations were systematically solved using the finite difference method and the Shooting technique implemented through MATLAB software. The outcomes revealed a reduction in fluid velocity as the inclined angle increased, highlighting the significant influence of thermal diffusion and Dufour effects on the convective transport flow. The study by Erik et al. [12] explored the dynamics of two-dimensional unsteady MHD flow within a viscous fluid confined between two parallel plates in motion. The authors considered scenarios where the plates moved both together and apart, representing a squeezing flow problem when moving together. By transforming the governing Navier–Stokes equations into a fourth-order nonlinear ordinary differential equation (ODE), they applied the homotopy analysis method to derive analytical solutions. The findings indicated that the flow exhibited significant sensitivity to both the magnetic field strength and the fluid density. The investigation into steady and unsteady MHD Couette flows between two parallel infinite plates was conducted by Hatami el al. [13] using the numerical Differential Quadrature Method (DQM) and the analytical Differential Transformation Method (DTM), respectively. In the coupled equations, they incorporated the viscosity effects of the two phases for both fixed and moving plates. Their findings indicated that, with a fixed magnetic source relative to the moving plate, an increase in the Hartmann number led to elevated velocity profiles for both phases. Conversely, an inverse trend was observed when the magnetic source was fixed relative to the fluid. Some studies on MHD and moving plates across various dimensions can be found in references [14-16].

The primary aim of this study is to examine the unsteady MHD convection of a radiating viscous incompressible electrically conducting fluid adjacent to a mobile permeable vertical plate within an environment characterized by variable temperature. The investigation utilizes the Laplace transform technique, implemented numerically through the finite difference method, to solve the

governing partial differential equations. The results are presented graphically and in tabular form, illustrating the impact of diverse emerging parameters on fluid velocity and temperature profiles, along with skin friction and Nusselt number.

The present article is organized as follows: Section 2 introduces the governing equations of the problem. Section 3 outlines the analytical approach employed, utilizing the Laplace Transform method. Section 4 elucidates the numerical approach. Subsequently, Section 5 presents and discusses the numerical computational results. Finally, Section 6 encapsulates the study's conclusions.

## 2. Mathematical formulation

Consider an unsteady laminar flow of a viscous incompressible electrically conducting fluid past an uniformly accelerating infinite vertical plate heating with variable temperature. The $x'$-axis is taken along the plate and $y'$-axis is normal to it. Initially, the plate and the adjacent fluid are at the same temperature $T'_\infty$ everywhere. At time $t' > 0$, heat is supplied from the surface of the plate to variable temperature, and the fluid is maintained temperature $T'_w$. A uniform inclined magnetic field $B_0$ is applied on plate with angle $\alpha$. The plate is infinite in length so all the physical quantities are function of $y'$ and $t'$ only. Thus, with usual Boussinesq approximation, the flow is governed by the following equations.

$$\frac{\partial u'}{\partial t'} - V\frac{\partial u'}{\partial y'} = \vartheta\frac{\partial^2 u'}{\partial y'^2} + g\beta(T' - T'_\infty) - \frac{\sigma B_0^2 \sin^2\alpha}{\rho}u' - \frac{\vartheta}{\kappa}u', \tag{1}$$

$$\frac{\partial T'}{\partial t'} - V\frac{\partial T'}{\partial y'} = \frac{k}{\rho C_p}\left(1 + \frac{16\sigma^* T'_\infty}{3kk^*}\right)\frac{\partial^2 T'}{\partial y'^2} + \frac{Q_0}{\rho C_p}(T' - T'_\infty), \tag{2}$$

with the initial and boundary conditions given as

$$\begin{aligned} &t' \le 0,\ u' = 0,\ T' = T'_\infty, && at \quad y' \ge 0,\\ &t' \ge 0,\ u' = \left(\frac{U^{2n+1}}{\vartheta^n}\right)t'^n, T' = T'_\infty + (T'_w - T'_\infty)\frac{U^2 t'}{\vartheta}, && at\ y' = 0,\\ &u' \longrightarrow 0, T' \longrightarrow T'_\infty, && as\ y' \longrightarrow \infty. \end{aligned} \tag{3}$$

The above equations are non-dimensionalised with the following variables and parameters;

$$u = \frac{u'}{U}, y = \frac{Uy'}{\vartheta}, R = \frac{16\sigma^* T'_\infty}{3kk^*}, \theta = \frac{T' - T'_\infty}{T'_w - T'_\infty}, M = \frac{\sigma\vartheta B_0^2 \sin^2\alpha}{\rho U^2}, K = \frac{\vartheta^2}{\kappa U^2},\ t = \frac{U^2 t'}{\vartheta}$$

$$S = \frac{V}{U}, Pr = \frac{\vartheta\rho C_p}{k}, U = \left(g\beta\vartheta(T'_w - T'_\infty)\right)^{\frac{1}{3}},\ Q = \frac{Q_0\vartheta}{U^2\rho C_p}, Gr = \frac{g\beta\vartheta(T'_w - T'_\infty)}{U^3},$$

$$M_1 = M + \frac{1}{K}. \tag{4}$$

Here $u'$ is the fluid velocity of fluid, $T'$the temperature of fluid, $T'_w$ is is the plate surface temperature, $T'_\infty$ is the free stream temperature, $U$ is the plate surface velocity coefficient, $V$ is the plate surface suction/injection velocity, $\vartheta$ the

coefficient of kinematic viscosity, $\kappa$ is the porous medium permeability, $\sigma$ is the fluid electrical conductivity, $M$ is the magnetic field parameter, $K$ is the porous medium parameter or Darcy number, $S$ is the suction /injection parameter, $Q$ is the heat source parameter, $Q_0$ is the heat source coefficient, $R$ is the thermal radiation parameter, $Gr$ is the thermal Grashof number, $Pr$ is the Prandtl number, $\rho$ is the fluid density, $C_p$ is the specific heat capacity at constant pressure, $k$ is the thermal conductivity, $\beta$ is volumetric thermal expansion coefficient, $g$ is acceleration due to gravity, $\sigma^*$ and $k^*$ are the Stefan-Boltzmann and mean absorption coefficients respectively. The governing equations in the non-dimensional form are obtained as

$$\frac{\partial u}{\partial t} - S\frac{\partial u}{\partial y} = \frac{\partial^2 u}{\partial y^2} + Gr\theta - M_1 u, \tag{5}$$

$$\frac{\partial \theta}{\partial t} - S\frac{\partial \theta}{\partial y} = \frac{(1+R)}{Pr}\frac{\partial^2 \theta}{\partial y^2} + Q\theta, \tag{6}$$

with the initial and boundary conditions given as

$$\begin{aligned} t \le 0, \quad u = 0, \ \theta = 0, \qquad & at \quad y \ge 0, \\ t \ge 0, u = t^n, \theta = t, \qquad & at \ y = 0, \\ u \longrightarrow 0, \quad \theta \longrightarrow 0, \qquad & as\ y \longrightarrow \infty. \end{aligned} \tag{7}$$

Other important quantities of interest are the skin friction $(C_f)$ and Nusselt number $(Nu)$ and they are given as follows:

$$C_f = -\frac{\partial u}{\partial y}\Big|_{y=0}, Nu = -\frac{\partial \theta}{\partial y}\Big|_{y=0}. \tag{9}$$

### 3. Analytical Approach: Laplace Transform Method

The Laplace transform of a given function $G(t,y)$ with respect to $t$ is defined as

$$\overline{G}(r,y) = \int_0^\infty G(t,y)e^{-rt}dt. \tag{9}$$

Taking Laplace transform of equations (5)-(7), we obtain

$$\frac{d^2\overline{u}}{dy^2} + S\frac{d\overline{u}}{dy} - (r + M_1)\overline{u} = -\frac{Gr}{r^2}exp\left(-\frac{y\left(S+\sqrt{S^2+4\delta(r+Q)}\right)}{2\delta}\right), \tag{10}$$

$$\frac{(1+R)}{Pr}\frac{d^2\overline{\theta}}{dy^2} + S\frac{d\overline{\theta}}{dy} - (r+Q)\overline{\theta} = 0, \tag{11}$$

subject to the following boundary conditions

$$\overline{u} = \frac{(n)!}{r^{n+1}}, \overline{\theta} = \frac{1}{r^2} \qquad at \ \ y = 0, \ \overline{u} \to 0, \overline{\theta} \to 0, \quad as \ \ y \to \infty. \tag{12}$$

Equations (10)- (11) are solved subject to boundary conditions (12) and we obtain

$$\overline{\theta} = \frac{1}{r^2}exp\left(-\frac{y\left(S+\sqrt{S^2+4\delta(r+Q)}\right)}{2\delta}\right). \tag{13}$$

$$\overline{u} = \left(\frac{n!}{r^{n+1}} + \frac{Gr}{(B^2 - BS - M_1 - r)r^2}\right) exp\left(-\left(\frac{S}{2} + \sqrt{\frac{S^2}{4} + M_1 + r}\right)y\right) - \frac{Gr*exp(-By)}{(B^2-BS-M_1-r)r^2}, \quad (14)$$

where $B = \frac{r}{2\delta} + \sqrt{\frac{S^2}{\delta^2} + \frac{r-Q}{\delta}}$.

Taking inverse Laplace transform of equation (13), we obtain

$$\theta = \left(\frac{t}{2} - \frac{y}{4c}\right)e^{-yc}erfc\left(\frac{y}{2\sqrt{t}} - ct\right) + \left(\frac{t}{2} + \frac{y}{4c}\right)e^{-yc}erfc\left(\frac{y}{2\sqrt{t}} + ct\right). \quad (15)$$

The inverse Laplace transform of equation (14) is given approximately as

$$u(y,t) = \frac{e^{\epsilon t}}{t}\left[\frac{1}{2}\overline{u}(y,\epsilon) + R_e\sum_{K=1}^{N}\overline{u}\left(y, \epsilon + \frac{iK\pi}{t}\right)(-1)^K\right], \quad (16)$$

where $R_e$ refers to the real part, $i = \sqrt{-1}$ is the imaginary number , $N$ is the number of terms used in the Riemann-sum approximation, $r$ is the Laplace transform variable, $n$ is the accelerating surface exponent, $\epsilon$ is the real part of the Bromwich contour that is used in inverting Laplace transform , $\delta = \frac{1+R}{Pr}$ and $c = \sqrt{\frac{S^2}{4\delta} - Q}$.

## 4. Numerical Approach: Finite Difference Method

A numerical resolution of the governing equations (5) - (6) which satisfied the initial and boundary conditions in equations (7) based on the finite difference method is implemented. The discretization is done as follows:

- Forward difference for temporal derivatives
- Central difference for space derivatives.

The model discretized equations are tackled iteratively on a computer using MAPLE software. The computations are carried out with a grid size of $\Delta y = 0.1$ and time step $\Delta t = 0.1$. The computations consider the default values: $S = O.1, Gr = 0.1, M = 0.1, K = 1, n = 1, R = 0.1, Pr = 0.71, Q = 0.1$ and $t = 0.5$.

## 5. Results and Discussion

The fundamental physical parameters govern the flow dynamics include the magnetic field parameter $(M)$, porous medium parameter $(K)$, Prandtl number $(Pr)$, suction parameter $(S)$, Grashof number $(Gr)$, thermal radiation parameter $(R)$, and heat source parameter $(Q)$. The figs. (1-7) illustrate the variations in velocity fields corresponding to different parameters, while figs. (8-12) depict the variations in temperature profiles associated with those parameters. The numerical values for skin friction and heat transfer rate are tabulated in table (1-2).

The graphical representation of the velocity profile for various values of parameter $(n)$, is presented in Fig.1. It is evident from the figure that as the value of $n$ increases, there is a notable decrease in velocity. Fig.2 illustrates the impact of time $(t)$, on the velocity profile. Notably, the observation reveals that an increment in time corresponds to a decline in velocity.

In Fig.3, we examine the impact of the Suction/Injection parameter $(S)$, on the velocity profile. The findings reveal a noteworthy correlation, showcasing that as the Suction/Injection parameter $(S)$, undergoes an increase, there is a corresponding decrease in the fluid velocity.

An increase in suction parameter signifies an enhanced fluid removal, resulting in a decrease in fluid velocity. Fig. 4 depicts the velocity response influenced by the thermal Grashof number $(Gr)$. Notably, as the Grashof number increases, there is a notable enhancement in the velocity profile. The heightened Grashof number signifies an augmentation in the thermal buoyancy forces, contributing to the intensified fluid motion evident in the expanded velocity profile.

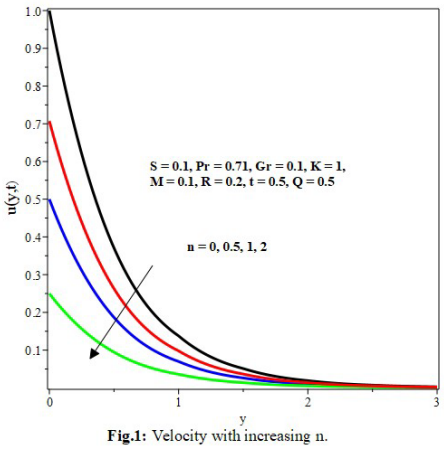


**Fig.1:** Velocity with increasing n.

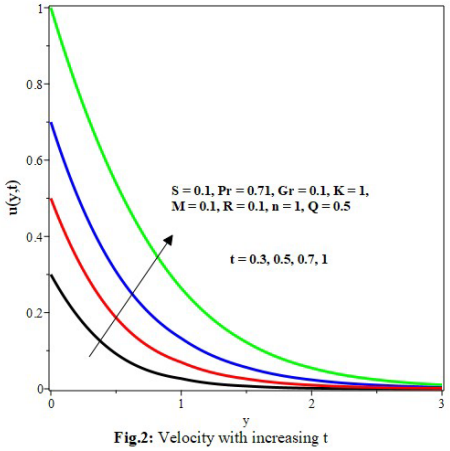


**Fig.2:** Velocity with increasing t

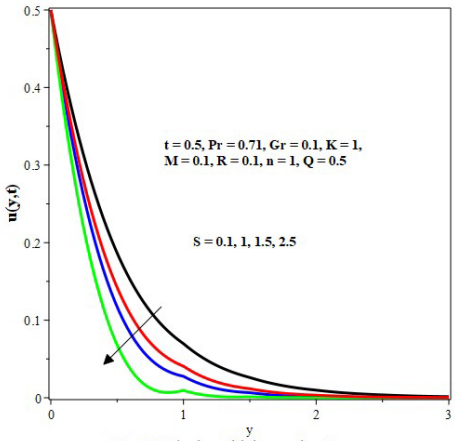


**Fig.3:** Velocity with increasing S

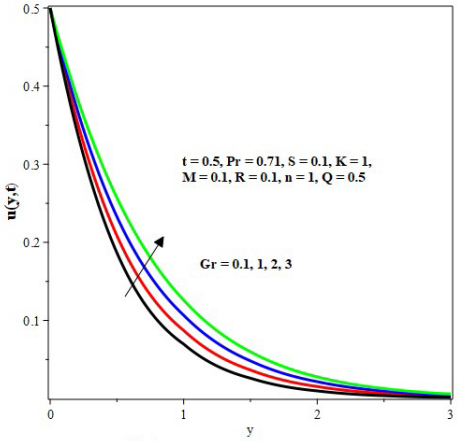


**Fig.4:** Velocity with increasing Gr

Fig.5 illustrates the impact of parameter $(K)$, on the velocity profile. The findings indicate that as the value of $K$, increases, the velocity profile has a concurrent rise. The elevated value of parameter $K$, corresponds to an amplified flow through the porous medium, leading to the observed increase in the velocity profile. The velocity profile depicted in Fig.6 illustrates the variations in velocity corresponding to changes in the Magnetic parameter $M$. It is evident from the graph that the velocity experiences a discernible decrease in response to the influence exerted by $M$. Fig.7 depicts the velocity profile in relation to the Prandtl number $(Pr)$. Notably, this figure illustrates a noteworthy trend wherein the velocity experiences a decrement with an increase in the Prandtl number.

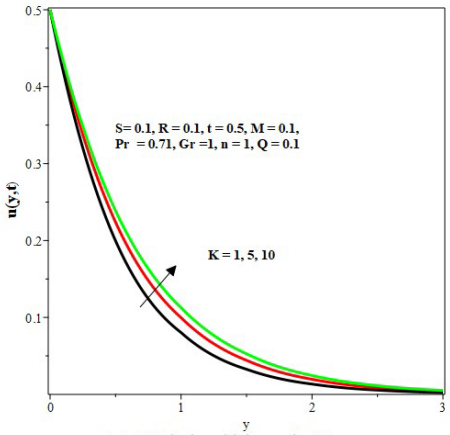

**Fig.5**:Velocity with increasing K

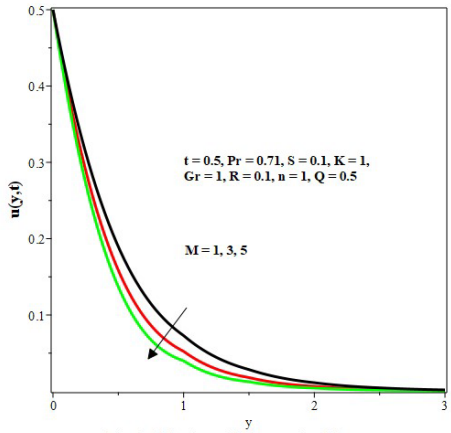

**Fig.6: Velocity with increasing M**

Fig.8 depicts the effects of increasing Prandtl number $(Pr)$ on the temperature profiles. As the Prandtl number rises, the thermal diffusivity is low compared to momentum diffusivity. This implies that heat diffuses slowly compared to momentum. This results in a thinner thermal boundary layer, steeper temperature gradients near surfaces, and potentially higher heat transfer efficiency in convective processes. These effects are crucial in designing systems for efficient thermal management, such as in heat exchangers, cooling systems, and various industrial processes. The observed slightly negative temperature at high Prandtl number $(Pr = 7.1)$ may be attributed to the cooling effects of the fluid resulting from a steep temperature gradient. Fig.9 demonstrates the temperature profile against the distance from the plate $(y)$ at different values of time $t$. The graph shows that as time t increases, the temperature also increases. Fig.10 demonstrates the influence of the radiation parameter $(R)$ on the temperature profile. The graph shows that as the value of $R$ increases, the temperature also increases. This is due to the fact that $R$ is responsible for the thermal boundary thickening, which leads to an increase in the temperature gradient at the surface. As a result, the heat transfer

rate decreases for increasing, causing the fluid to lose heat energy from the flow region. This results in an increase in temperature as the value of R increases.

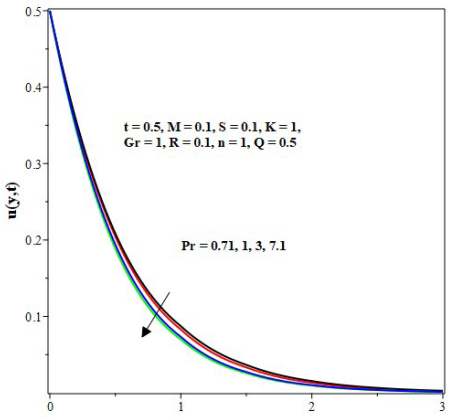


**Fig.7:** Velocity with increasing Pr

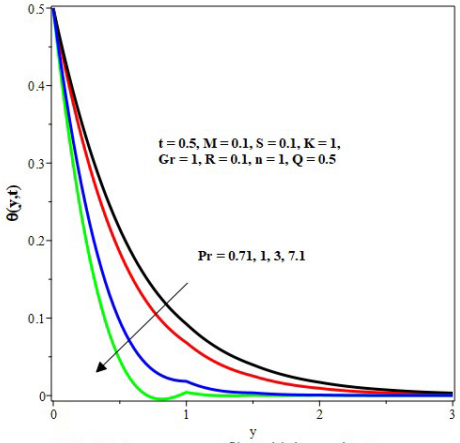


**Fig.8:** Temperature profiles with increasing Pr

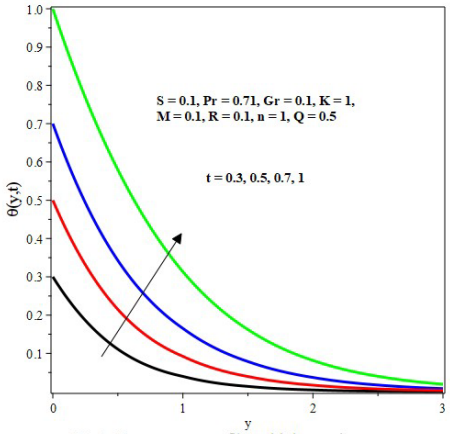


**Fig.9**: Temperature profiles with increasing t

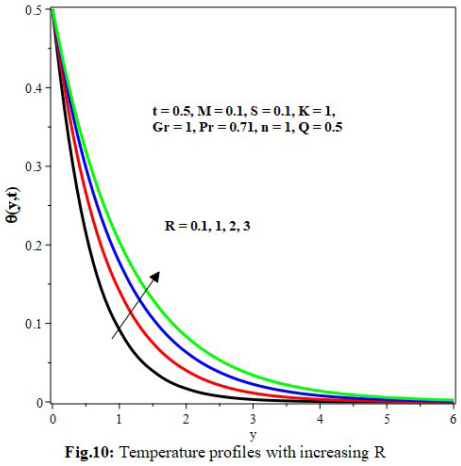


**Fig.10:** Temperature profiles with increasing R

Fig.11 portrays the influence of various suction parameters $S$ on temperature concerning y. The figure distinctly illustrates that the temperature reaches its maximum at the plate, undergoes a rapid decline in proximity to the plate, and tends towards zero asymptotically. In Fig.12, the impact of the heat source parameter $Q$ on the temperature field is depicted. The results suggest that as the source parameter increases, there is a corresponding rise in fluid temperature.

The computed coefficient of skin friction at time $t = 0.5$ along with the impact of diverse physical parameters, is presented in Table 1. An examination of the table reveals that skin friction diminishes with an escalation of parameters $n, M, R$ and $Q$, while it increases with rising values of parameters $S$ and $K$. Table 2 depicts the numerical values of the Nusselt number at time $t = 0.5$ for various parameters. The table shows that the value of the Nusselt number decreases with an increase in $R$ and $Q$, while it increases with an increase in $Pr$ and $S$.

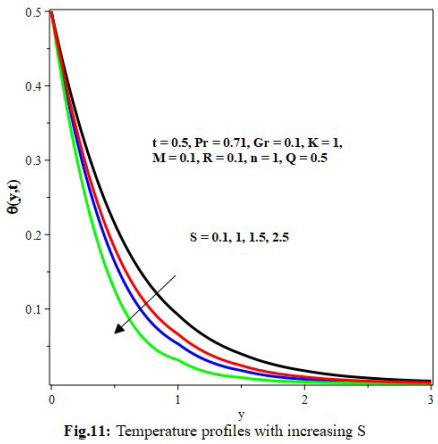


**Fig.11:** Temperature profiles with increasing S

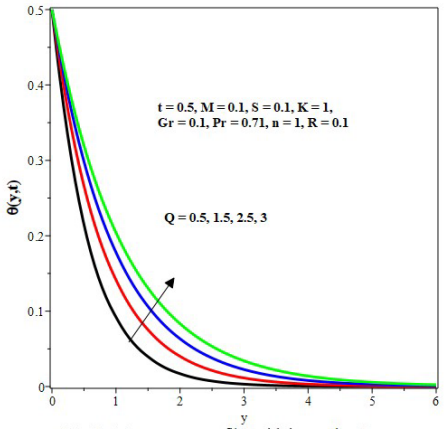


**Fig.12:** Temperature profiles with increasing Q

*Table 1*

**Computations showing the parameters effects on skin friction when $t = 0.5$.**

| $n$ | $S$ | $Gr$ | $M$ | $K$ | $Pr$ | $R$ | $Q$ | $C_f$ |
|---|---|---|---|---|---|---|---|---|
| 0 | 0.1 | 0.1 | 0.1 | 1.0 | 0.71 | 0.1 | 0.1 | 1.9706064 |
| 0.5 | 0.1 | 0.1 | 0.1 | 1.0 | 0.71 | 0.1 | 0.1 | 1.3907698 |
| 1.0 | 0.1 | 0.1 | 0.1 | 1.0 | 0.71 | 0.1 | 0.1 | 0.9807633 |
| 1.0 | 0.5 | 0.1 | 0.1 | 1.0 | 0.71 | 0.1 | 0.1 | 1.0557947 |
| 1.0 | 1.0 | 0.1 | 0.1 | 1.0 | 0.71 | 0.1 | 0.1 | 1.1553758 |
| 1.0 | 0.1 | 0.5 | 0.1 | 1.0 | 0.71 | 0.1 | 0.1 | 0.9444447 |
| 1.0 | 0.1 | 1.0 | 0.1 | 1.0 | 0.71 | 0.1 | 0.1 | 0.8991094 |
| 1.0 | 0.1 | 0.1 | 0.5 | 1.0 | 0.71 | 0.1 | 0.1 | 1.0072197 |
| 1.0 | 0.1 | 0.1 | 1.0 | 1.0 | 0.71 | 0.1 | 0.1 | 1.0378089 |
| 1.0 | 0.1 | 0.1 | 0.1 | 5.0 | 0.71 | 0.1 | 0.1 | 0.9215297 |
| 1.0 | 0.1 | 0.1 | 0.1 | 10 | 0.71 | 0.1 | 0.1 | 0.9135056 |
| 1.0 | 0.1 | 0.1 | 0.1 | 1.0 | 3.0 | 0.1 | 0.1 | 0.9855481 |
| 1.0 | 0.1 | 0.1 | 0.1 | 1.0 | 7.1 | 0.1 | 0.1 | 0.9877414 |
| 1.0 | 0.1 | 0.1 | 0.1 | 1.0 | 0.71 | 0.5 | 0.1 | 0.9798364 |
| 1.0 | 0.1 | 0.1 | 0.1 | 1.0 | 0.71 | 1.0 | 0.1 | 0.9789513 |
| 1.0 | 0.1 | 0.1 | 0.1 | 1.0 | 0.71 | 0.1 | 0.5 | 0.9804976 |
| 1.0 | 0.1 | 0.1 | 0.1 | 1.0 | 0.71 | 0.1 | 1.0 | 0.9800231 |

*Table 2*

**Computations showing the parameters effects on Nusselt number when $t = 0.5$.**

| $R$ | $S$ | $Q$ | $Pr$ | $Nu$ |
|---|---|---|---|---|
| 0.1 | 0.1 | 0.1 | 0.71 | 0.749752 |
| 0.5 | 0.1 | 0.1 | 0.71 | 0.654130 |
| 1.0 | 0.1 | 0.1 | 0.71 | 0.573674 |
| 0.1 | 0.5 | 0.1 | 0.71 | 0.806960 |
| 0.1 | 1.0 | 0.1 | 0.71 | 0.883380 |
| 0.1 | 0.1 | 0.5 | 0.71 | 0.716829 |
| 0.1 | 0.1 | 1.0 | 0.71 | 0.671609 |
| 0.1 | 0.1 | 0.1 | 3.0 | 1.266099 |
| 0.1 | 0.1 | 0.1 | 7.1 | 1.540968 |

## 6. Conclusions

The present study investigated the effects of various parameters on the velocity and temperature profiles, as well as the skin friction and Nusselt number. These parameters include $M, Gr, Pr, S, R, K, Q$ and $n$. The results show that skin friction increases with an increase in the parameter values of $S, M$ and $Pr$, but decreases with an increase in the parameter values of $n, Gr, K, R$ and $Q$. A boost in the values of $S$ and $Pr$ augment the Nusselt number, while a rise in $R$ and $Q$ lessens it. Generally, the fluid velocity and temperature attained their maximum value at the plate surface and thereafter decreased to the free stream values satisfying the prescribed boundary conditions. An increase in $t, Gr$ and $K$ boosts the velocity profiles, while a rise in $n, S, M$ and $Pr$ lessens it. The fluid temperature rises with $R, Q$ and $t$ but declines with $S$ and $Pr$.

## R E F E R E N C E S


[1]. *G. G. Stokes*, On the Effect of the Internal Friction of Fluids on the Motion of Pendulums. Transactions of the Cambridge Philosophical Society, **9(8)**(1851).

[2]. *K. J. Bassant and A.A. Clement,* MHD Natural convection flow of fluids of different Prandtl numbers in the Stokes problem for vertical plate J. Phys. Soc. Jpn. **81**(2012)064401.

[3]. *B.P. Reddy and O. D. Makinde,* Newtonian heating effect on heat absorbing unsteady MHD radiating and chemically reacting free convection flow past an oscillating vertical porous plate. International Journal of Applied Mechanics and Engineering, **Vol.27(1)**(2022), 168-187.

[4]. *M. Sulemana, I.Y. Seini and O.D. Makinde,* Hydrodynamic Boundary Layer Flow of Chemically Reactive Fluid over Exponentially Stretching Vertical Surface with Transverse Magnetic Field in Unsteady Porous Medium. Journal of Applied Mathematics, **Vol. 2022**(2022), Article ID 7568695 (11pages).

[5]. *A. S. Eegunjobi, O.D. Makinde, and S. Jangili,* Unsteady MHD Chemically Reacting and Radiating Mixed Convection Slip Flow Past a Stretching Surface in a Porous Medium. Defect and Diffusion Forum. **Vol.377,** ISSN: 1662-9507(2017), pp 200-210.

[6]. *C.K. Ajay, M.Ajay Kumar and A.H. Srinivasa,* The effects of thermal radiation, internal heat generation (absorption) on unsteady MHD free convection flow about a truncated cone in presence of pressure work, Materials Today: Proceedings, https://doi.org/10.1016/j. matpr.2023.05.632

[7]. *Bodhinanda Chandra, Ryota Hashimoto, Shinnosuke Matsumi, Ken Kamrin and Kenichi Soga*, Stabilized mixed material point method for incompressible fluid flow analysis. Computer Methods in Applied Mechanics and Engineering **419**(2024), 116644.

[8]. *Sohail Nadeem, Rehan Akber, Hassan Ali Ghazwani, Jehad Alzabut and Ahmed M. Hassan,* Numerical computations for convective MHD flow of viscous fluid inside the hexagonal cavity having sinusoidal heated walls. Results in Physics **56**(2024), 107229.

[9]. *Wei An, Jian Yu, Hongqiang Lyu and Xuejun Liu,* An R-adaptive algorithm based on self-organizing maps for solving incompressible flows with high-order discontinuous Galerkin methods. Computers and Fluids **270**(2024),106160.

[10]. *Tahera Begum, Geetan Manchanda, Arshad Khan, Naseem Ahmad,* On numerical solution of boundary layer flow of viscous incompressible fluid past an inclined stretching sheet in porous medium and heat transfer using spline technique. Methods **10**(2023),102035.

[11]. *Hasanuzzaman Md., Mahamudul Hassan Milon, Md.Mosharrof Hossain and Md. Asaduzzaman,* Dufour and thermal diffusion effects on time-dependent natural MHD convective transport over an inclined porous plate. International Journal of Thermofluids **21**(2024),100572.

[12]. *Erik Sweet, K. Vajravelu, A.V.G. Robert and I. Pop,* Analytical solution for the unsteady MHD flow of a viscous fluid between moving parallel plates. Commun Nonlinear Sci Numer Simulat **16**(2011), 266-273.

[13]. *M. Hatami, K.H.Hosseinzadeh, G. Domairrand M.T. Behnamfar,* Numerical study of MHD two-phase Couette flow analysis for fluid-particle suspension between moving parallel plates. Journal of the Taiwan Institute of Chemical Engineers b(2014), 2238-2245.

[14]. *M. Z. Stamenkovic Ivojin and D. Dragis Nikodijevi,* MHD Flow and Heat Transfer of Two Immiscible Fluids between. Moving Plates. Transactions of the Canadian Society for Mechanical Engineering, b(2010), No. 3-4.

[15]. *Mohammadreza Azimi and Rouzbeh Riazi,* MHD unsteady GO-water-squeezing nanofluid flow-heat and mass transfer between two infinite parallel moving plates: analytical investigation. Indian Academy of Sciences. Sadhana **Vol. 42, No. 3**(2017), pp. 335-34.

[16]. *R. Delhi Babu, S. Ganesh and M. Anish,* Steady two-dimensional MHD stokes flow between two parallel plates under angular velocity with one plate moving uniformly and the other plate at rest and uniform suction at the stationary plate. International Journal of Ambient Energy **vol. 43, no. 1**(2022), 741-744.